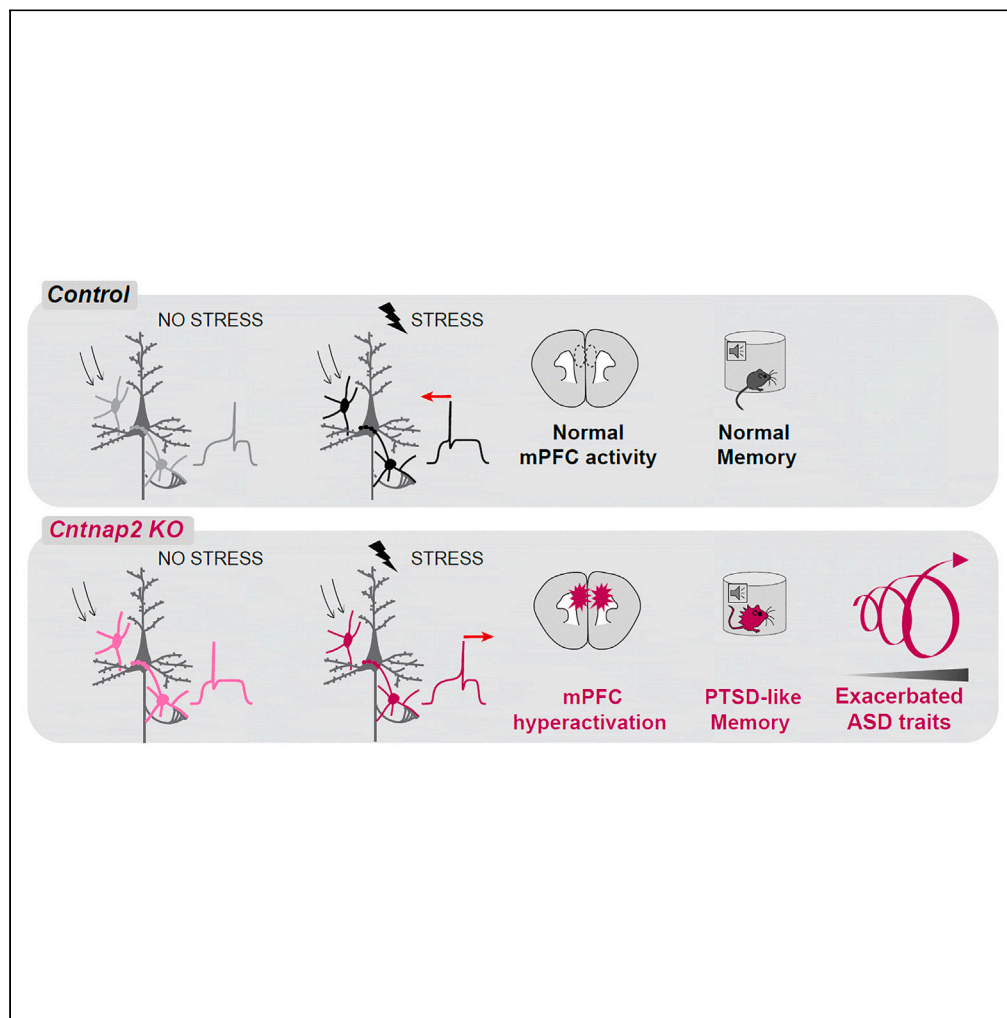## Article

Parvalbumin interneuron activity in autism underlies susceptibility to PTSD-like memory formation

Alice Shaam Al Abed, Tiarne Vickie Allen, Noorya Yasmin Ahmed, ..., Aline Marighetto, Aline Desmedt, Nathalie Dehorter

shaam.alabed@anu.edu.au (A.S.A.A.)
nathalie.dehorter@anu.edu.au (N.D.)

Highlights

This study demonstrates a reciprocal relationship between ASD and PTSD-like memory

Recontextualization constitutes a behavioral strategy to treat PTSD-related amnesia

Recontextualization rescues PTSD-like memory in ASD and aggravation of core traits

Prefrontal parvalbumin interneurons are a target to treat PTSD-like memory in ASD

iScience

Article

Parvalbumin interneuron activity in autism underlies susceptibility to PTSD-like memory formation

Alice Shaam Al Abed,[1,2,5,][*] Tiarne Vickie Allen,[1] Noorya Yasmin Ahmed,[1,2] Azza Sellami,[3,4] Yovina Sontani,[1] Elise Caitlin Rawlinson,[1] Aline Marighetto,[3,4] Aline Desmedt,[3,4] and Nathalie Dehorter[1,2,][*]

SUMMARY

A rising concern in autism spectrum disorder (ASD) is the heightened sensitivity to trauma, the potential consequences of which have been overlooked, particularly upon the severity of the ASD traits. We first demonstrate a reciprocal relationship between ASD and post-traumatic stress disorder (PTSD) and reveal that exposure to a mildly stressful event induces PTSD-like memory in four mouse models of ASD. We also establish an unanticipated consequence of stress, as the formation of PTSD-like memory leads to the aggravation of core autistic traits. Such a susceptibility to developing PTSD-like memory in ASD stems from hyperactivation of the prefrontal cortex and altered fine-tuning of parvalbumin interneuron firing. Traumatic memory can be treated by recontextualization, reducing the deleterious effects on the core symptoms of ASD in the *Cntnap2* KO mouse model. This study provides a neurobiological and psychological framework for future examination of the impact of PTSD-like memory in autism.

INTRODUCTION

Autism spectrum disorder (ASD) is a neurodevelopmental disorder caused by a combination of genetic and environmental factors that impair neuronal circuit function and lead to behavioral difficulties, such as altered social behavior and repetitive movements.[1,2] Beyond the core traits, people with ASD present with cognitive defects, including hyper-reactivity to sensory stimuli,[3] abnormal fear conditioning,[4] and altered declarative memory.[5] Such a combination of impairments suggests a potential predisposition for developing post-traumatic stress disorder (PTSD), in which extreme stress induces an altered memory of an event.[1,6] In line with recent studies in humans positing a co-occurrence of these two disorders,[7–9] ASD and PTSD display common behavioral features including impaired emotional regulation, cognitive rigidity, and fragmented autobiographical memory.[5] Yet, the link between the two disorders remains poorly explored. This is critical to address, as there is a pressing need not only for explaining the occurrence of traumatic stress in autism but also for understanding the mechanisms underlying the unique perception of traumatic events in this condition.[7]

As a crucial component of fear memory circuitry,[10] the medial prefrontal cortex (mPFC) controls downstream structures including the hippocampus and the amygdala to drive executive functions such as short-term memory and reasoning.[11,12] The dysfunction of the mPFC has been shown in both ASD[13] and PTSD,[14] suggesting that this structure represents a common node where cellular alterations may contribute to the emergence of these disorders. The mPFC contains fast-spiking parvalbumin-expressing interneurons (PV-INs) that provide critical inhibitory control and maintain the excitation/inhibition balance in cortical circuits. These cells are required for adapted fear memorization[11] and normal sensory function.[15] They play an essential role in stress-related disorders,[16] as well as in ASD, where they drive aberrant cortical activity.[15,17,18] Together, PV-INs represent cellular targets for normalizing functional connectivity and behavior in ASD, as their excitation has been shown to rescue social impairments in the contactin-associated protein 2 knock out (*Cntnap2* KO) mouse model, which recapitulates the core symptoms of ASD.[18,19] However, there is an urgent need to investigate the extent to which PV-INs are involved in the cognitive deficits and their role in tuning cortical activity in response to stress in ASD.

In this study, we aimed to investigate key cellular and molecular mechanisms involved in interneuron adaptation to stress, that impact both medial prefrontal cortex activity and memory formation, and in turn contribute to the pathophysiology of ASD.

[1]Eccles Institute of Neuroscience, John Curtin School of Medical Research, The Australian National University, Canberra, ACT, Australia
[2]The Queensland Brain Institute, The University of Queensland, Brisbane, QLD, Australia
[3]Neurocentre Magendie, Physiopathologie de la plasticité neuronale, U1215, INSERM, F-33000 Bordeaux, France
[4]Université de Bordeaux, F-33000 Bordeaux, France
[5]Lead contact
*Correspondence: shaam.alabed@anu.edu.au (A.S.A.A.), nathalie.dehorter@anu.edu.au (N.D.)
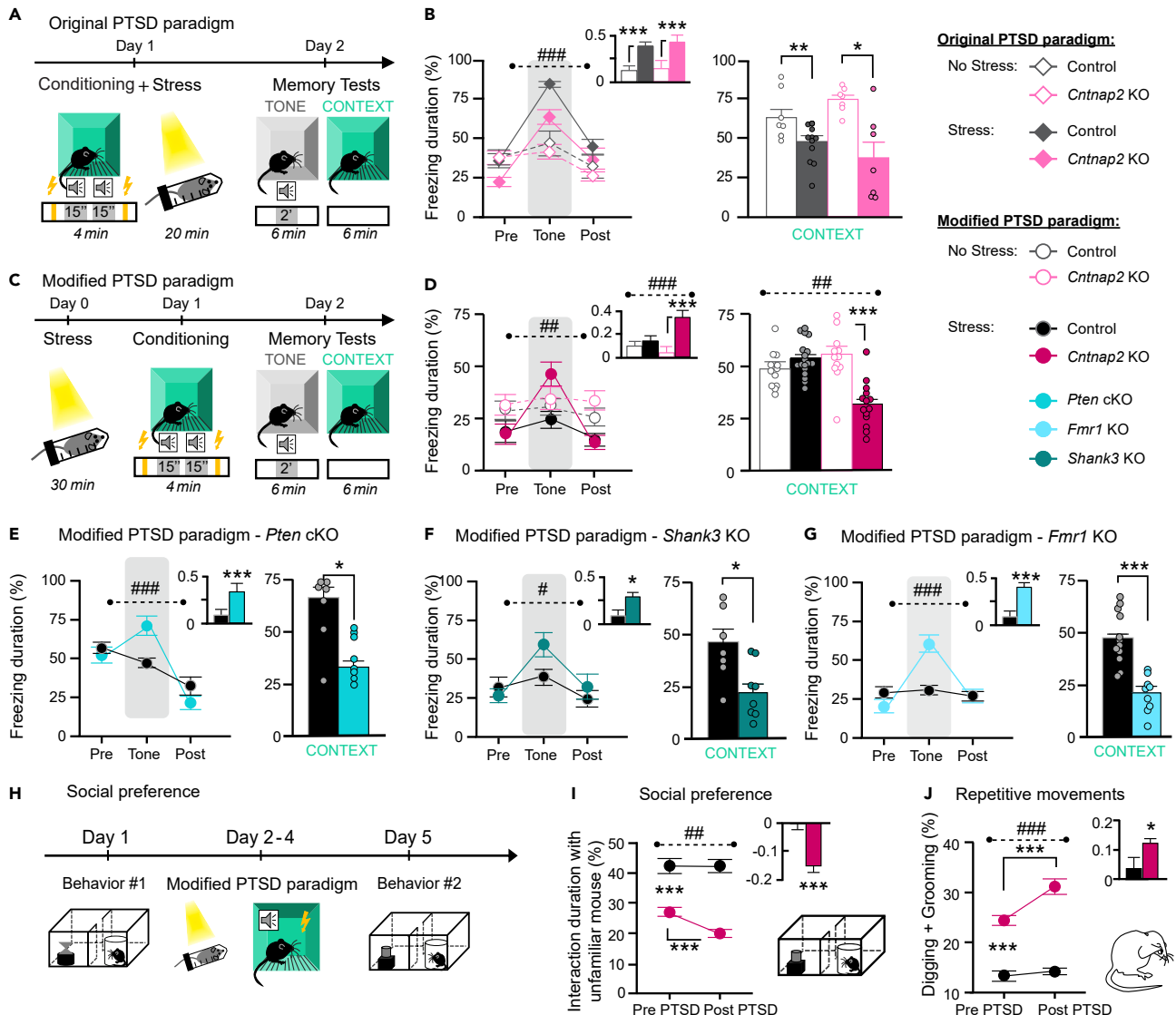https://doi.org/10.1016/j.isci.2024.109747

Figure 1. *Cntnap2* KO mice display traumatic memory profile after non-traumatic stress

(A) Behavioral design of the original PTSD paradigm.

(B) Mean fear responses of non-stressed and stressed control and KO groups in the original PTSD paradigm, measured as percentage of freezing duration before (pre), during (tone), and after (post) presentation of the tone (left; $p < 0.001$; tone ratio (inset): $p < 0.001$) and context tests (right; $p < 0.05$); $n = 7$ Non stressed Control (white fill) & 11 Stressed Control mice (gray fill); $n = 7$ Non stressed *Cntnap2* KO (white fill) and 7 Stressed *Cntnap2* KO mice (pink fill); #: significant stress x freezing block repeated measures interaction, $p < 0.001$.

(C) Behavioral design of the modified PTSD paradigm.

(D) Mean fear responses of non-stressed and stress groups in the modified PTSD paradigm, measured as percentage of freezing duration before (pre), during (tone) and after (post) the tone (left; #: significant genotype x stress x freezing block repeated measures interaction, $p < 0.01$.; tone ratio (inset): #: significant genotype × stress interaction, $p < 0.001$)) and context tests (right; ns); $n = 16$ Control (gray) and 13 *Cntnap2* KO mice (pink); right; $p < 0.001$; $n = 24$ Control stressed (black) and 24 *Cntnap2* KO stressed (magenta); #: significant genotype x stress interation, $p < 0.001$)); (E) Fear responses in stressed *Pten* control ($n = 7$), *Pten* cKO (cyan; $n = 8$) mice, (tone test (left); #: significant genotype x freezing block repeated measures interaction, $p < 0.0001$; tone ratio (inset): $p = 0.0004$; context test (right): $p = 0.0242$).

(F) Fear responses in stressed *Shank3* control ($n = 7$), *Shank3* KO (teal; $n = 8$) mice, (tone test (left); #: significant genotype x freezing block repeated measures interaction, $p = 0.0330$; tone ratio (inset): $p = 0.0297$; context test (right): $p = 0.0100$).

(G) Fear responses in stressed *Fmr1* control ($n = 12$), *Fmr1* KO (light blue; $n = 9$) mice (tone test (left); #: significant genotype x freezing block repeated measures interaction, $p < 0.0001$; tone ratio (inset): $p < 0.001$; context test (right): $p < 0.001$).

(H) Timeline of the assessment of autistic traits before and after the modified PTSD paradigm.

Figure 1. *Continued*

(I) Left; Social preference test before and after the modified PTSD paradigm: duration of interaction with an unfamiliar mouse in stressed control (black; *n* = 11) and *Cntnap2* KO mice (magenta; *n* = 14; Control vs. KO: *p* < 0.001; Pre- vs. Post-PTSD in Control: ns and in KO: *p* < 0.001; #: significant genotype x repeated measure (sessions), *p* < 0.0001) mouse interaction index (inset): *p* < 0.001). Bottom right: 2-chamber arena for social preference testing.

(J) Repetitive movements before and after the modified PTSD paradigm (digging and grooming; *n* = 11 Control & 18 KO; Control vs. KO: #: significant genotype x repeated measure (sessions), *p* < 0.001; Pre- and Post-PTSD in Control: ns and in *Cntnap2* KO: *p* < 0.001; ratio (inset): *p* < 0.05). Data presented as mean ± SEM. ***: *p* < 0.001; **: *p* < 0.01; *: *p* < 0.05 from two-way ANOVA (stress x genotype); #: interaction significance. See also Figures S1–S3. See table for precise statistics.

RESULTS

Stress in memorization and autistic traits

A cardinal feature of PTSD is the development of a maladaptive memory of a traumatic event.[20] Here, we studied PTSD-like memory formation in the *Cntnap2* KO mouse model, using a contextual fear conditioning paradigm, paired with restrain stress, as a model of PTSD-like memory.[21,22] This paradigm combines two auditory tones unpaired to two mild electric foot shocks (Figure 1A; Day 1), in which the tones do not predict the foot shocks. As such, the environment or "context" of the conditioning session becomes the only relevant predictor of the threat. We found that non-stressed control mice developed an adapted contextual fear memory, characterized by a low fear of the tone (i.e., tone test; Figure 1A, Day 2; Figure 1B left panel), combined with a strong fear of the conditioning context (i.e., context test; Figure 1A, Day 2; Figure 1B right panel). In contrast, submitting control mice to a 20 min restraint stress immediately after the conditioning led to the development of a maladaptive memory, consisting of a strong fear of the tone, and marginal fear of the conditioning context (Figure 1B). This abnormal memory profile mimics PTSD-related memory, by combining intrusive sensory hypermnesia for a salient, yet irrelevant element of the trauma (the tone), with a partial amnesia of the surrounding context.[1,6,23] Strikingly, *Cntnap2* KO mice displayed the same memory profiles as control mice (Figure 1B). While non-stressed *Cntnap2* KO mice were able to form adapted contextual memory, stressed *Cntnap2* KO mice showed fear of the irrelevant tone, and low fear of the conditioning context. This demonstrates that, as control mice, *Cntnap2* KO mice develop PTSD-like memory after a stressful event.

It is well-known that ASD is characterized by difficulties coping with stress.[3] We hence reasoned that PTSD-like memory could be triggered in *Cntnap2* KO mice with levels of stress that do not affect control mice. Utilizing a modified version of the original PTSD-like memory protocol,[21,22] we subjected mice to a 30 min restraint stress 24 h before conditioning (Figure 1C). In this paradigm, both non-stressed control and *Cntnap2* KO mice displayed an adaptive contextual fear memory 24 h post-conditioning (Figure 1C, Day 2; Figure 1D). In contrast, an independent group of stressed *Cntnap2* KO mice showed strong and specific fear response to the tone combined with low freezing to the conditioning context, while stressed control mice demonstrated normal contextual fear memory (Figure 1D). This abnormal fear memory recapitulated all features of PTSD-like memory (STAR methods): partial fear generalization (i.e., fear of a similar, yet non-identical, salient element of the traumatic event; Figure S1A) and persisting across time (Figure S1B). Furthermore, we found no difference in the reactivity to the electric foot shock or the tone presentation between control and *Cntnap2* KO mice following stress and fear conditioning (Figure S1C), indicating that PTSD-like memory did not stem from altered sensory processing.[3] To confirm that this profile was a feature of the autistic condition and not due to specific features of the *Cntnap2* KO mouse model, we tested the protocol (i.e., restraint stress and unpaired fear conditioning) in three additional mouse models of ASD: The phosphatase and tensin homolog conditional knockout (*Pten*$^{F/F}$; *Emx1*$^{Cre/+}$: *Pten* cKO), the *Shank* 3 KO, and the Fragile-X *Fmr1* KO mouse models of autism.[24,25] Following this paradigm, *Pten* cKO, *Shank3* KO, and *Fmr1* KO mice displayed a traumatic memory profile (Figures 1E–1G, respectively), overall proving a general vulnerability to developing PTSD-like memory in autism.

Given the similar behavioral features of both PTSD and ASD conditions (impaired emotional regulation and cognitive rigidity[26]), we hypothesized that PTSD-like memory formation could exacerbate ASD-related traits. We therefore quantified social (Figures 1H, 1I, S2A, and S2B) and repetitive behaviors (i.e., digging and grooming; Figures 1J, S2C, and S2D) of *Cntnap2* KO mice compared to control mice. As previously described, *Cntnap2* KO mice displayed decreased exploration of an unfamiliar animal (Figures 1I, S2A, S2B, S2E, S2F, and S2G), and increased repetitive movements (Figures 1J, S2C, and S2D). Remarkably, PTSD-like memory formation in *Cntnap2* KO mice aggravated the severity of both core autistic traits, as observed in both the classic (Figures S2H–S2J) and modified PTSD protocols (Figures 1I and 1J). In contrast, fear conditioning alone or stress alone (Figures S2B–S2G) had no effect upon these traits in neither control nor C*ntnap2* KO mice. The observed effects of PTSD-like memory upon autistic traits did not stem from altered locomotion, as the total interaction time with the animal and the object (Figure S2F) or the time spent moving (Figure S2G) was not differentially affected by PTSD-like memory formation in *Cntnap2* KO mice compared to control mice. This exacerbation was maintained for 3 weeks post-conditioning (Figures S2I and S2J).

We next examined the malleability of the pathological memory developed in ASD conditions to determine whether it was possible to rescue PTSD-like memory in ASD mice. We used a behavior-based rehabilitation strategy called "recontextualization",[22,23,27] which has been shown to successfully normalize PTSD-like memory in control mice.[22] We re-exposed the *Cntnap2* KO mice with PTSD-like memory to the original tone in the conditioning context with no foot shock (Figure 2A). While the stressed *Cntnap2* KO mice replicated the amnesia to the conditioning context, followed by a strong and high fear response to the tone during the recontextualization session (Figure 2B), 24 h later they exhibited normal, contextualized fear memory (Figure 2C). Importantly, restoring normal memory improved social behavior and decreased repetitive movements to levels close to that of control mice (Figures 2D, 2E, and S2K–S2O). To note, we did not find any sexual dimorphism regarding the impact of stress in fear conditioning (Figures S3A and S3B), or the aggravation of the core autistic traits
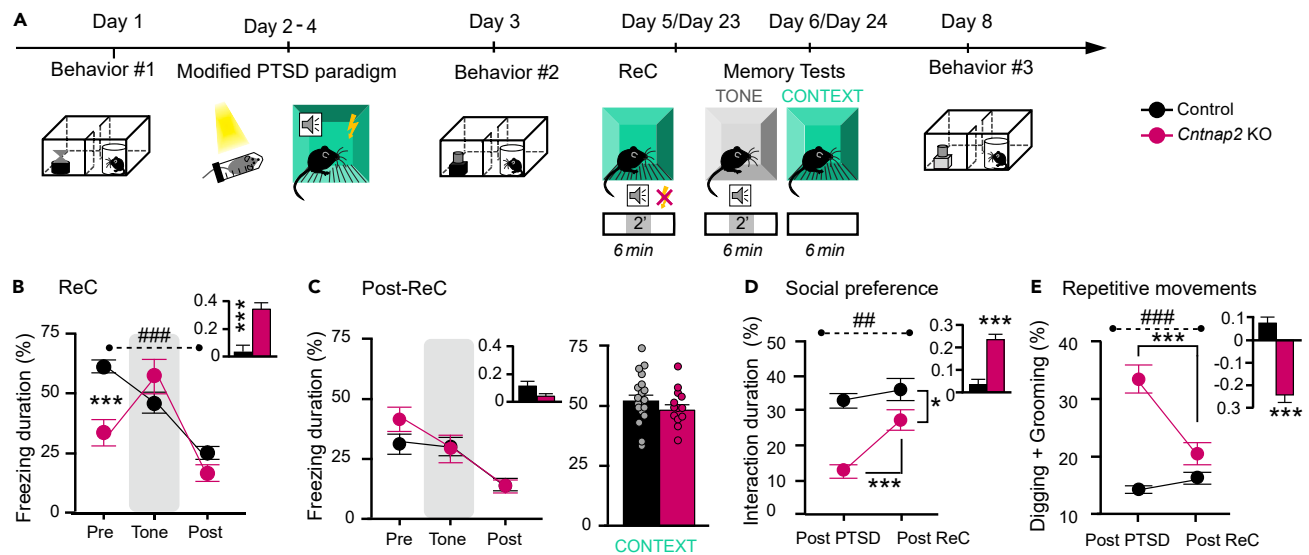
Figure 2. Recontextualization to normalize PTSD-like memory in the *Cntnap2* KO mouse model of ASD

(A) Schematics of the recontextualization (ReC) session and subsequent memory tests.

(B) Fear responses during the ReC session (n = 19 control stress + FC and 14 *Cntnap2* KO stress + FC; Pre: $p < 0.001$; #: genotype x freezing block repeated measures interaction: $p < 0.001$; Tone ratio during ReC (inset): $p < 0.001$).

(C) Fear responses post-ReC session, for the tone (left) and context (right) tests (n = 19 Control and 14 *Cntnap2* KO mice; ns).

(D) Social preference before and after ReC protocol (n = 10 Control and 12 KO; #: Genotype x Repeated measure sessions interaction $p < 0.01$; Post-PTSD vs. Post-ReC: ns in Control & $p < 0.001$ in KO; Post ReC Control vs. KO $p < 0.05$); between-session interaction ratio (inset) ($p < 0.001$).

(E) Repetitive movements before and after ReC protocol (n = 10 Control & 16 KO; #: Genotype x Repeated measure sessions interaction $p < 0.001$; Post-PTSD vs. Post-ReC: ns in Control and $p < 0.001$ in KO); Inset represents the between-session repetitive movement ratio ($p < 0.001$). Data presented as mean ± SEM. ***: $p < 0.001$; **: $p < 0.01$; *: $p < 0.05$ from 1-way ANOVA; #: interaction significance between repeated measures and genotype. See also Figures S2 and S3. See table for precise statistics.

with PTSD-like memory formation in the *Cntnap2* KO mice (Figures S3C and S3D). Together, these data demonstrate that while PTSD-like memory exacerbates the core traits of ASD, it is possible to manipulate this pathological memory and subsequently alleviate ASD-related behaviors. Therefore, it provides evidence for a reciprocal relationship between PTSD-like memory and ASD, in the *Cntnap2* KO mice.

mPFC hyperactivation elicits PTSD-like memory

Alterations in the activity of the medial prefrontal cortex (mPFC) have been previously described in both PTSD[14] and ASD.[13,28] Overall, decreased PFC functional activation to stressful and trauma-related cues, has been found in PTSD patients,[29] while hyperactivity of the principal neurons has been described in ASD.[13] To uncover the impact of PTSD-like memory formation in ASD, we analyzed neuronal activation induced by re-exposure to the conditioning context using the cell activity marker c-Fos.[21] While there was no difference in cFos-positive cell density at the basal level between control and *Cntnap2* KO mice (i.e., naive non-trained; Figure 3A, left panel), stressed *Cntnap2* KO mice presented more c-Fos positive cells in the mPFC than stressed control mice (Figures 3A and 3B). In particular, we found that the infralimbic (IL) region of the mPFC supports this phenotype, as opposed to the prelimbic (PL) area, where no significant elevation in cFos+ cell number was detected (Figure 3A, right panel). This increase in IL cell activation was associated to alterations in downstream structures involved in the fear memory circuitry.[10] We found a significant decrease in c-Fos-positive cells in the amygdala and hippocampus of stressed *Cntnap2* KO mice following re-exposure to the conditioning context, compared to control mice (Figures S4A and S4B). Interestingly, limited cFos activation was detected in PV-INs (Figures 3B and 3C), with significantly lower cFos expressing PV-INs only in naive *Cntnap2* KO mice, compared to control mice. This suggests that the cFos increase observed after context test was specific to putative pyramidal cells (Figure 3A).

To further characterize the causal relationship between mPFC activity and PTSD-like memory formation, we performed *in vivo* optogenetic modulation of the pyramidal cells of the mPFC during the modified fear conditioning protocol (Figures 3D, S4C, and S4D). We found that optogenetic stimulation of the prefrontal cortical *CaMKII*-positive pyramidal cells via channelrhodopsin (ChR2) activation in stressed control mice was sufficient to trigger traumatic memory formation (Figure 3E). Similarly, optical stimulation of the mPFC pyramidal cells in non-stressed *Cntnap2* KO mice induced PTSD-like memory (Figure S4E). Conversely, optogenetic inhibition of the mPFC pyramidal cells via Archaerhodopsin (ArchT) activation in stressed *Cntnap2* KO mice during conditioning successfully prevented PTSD-like memory formation (Figure 3F). Together, these data indicate that stress-induced mPFC hyperactivation in ASD underlies PTSD-like memory formation.
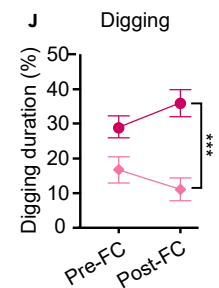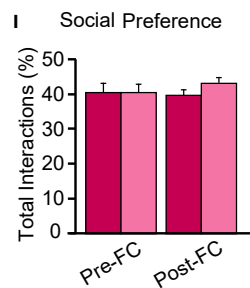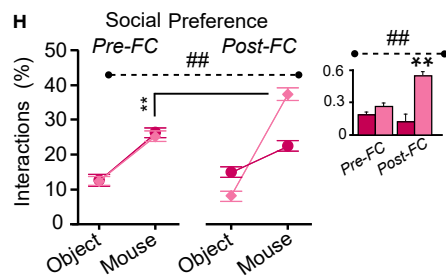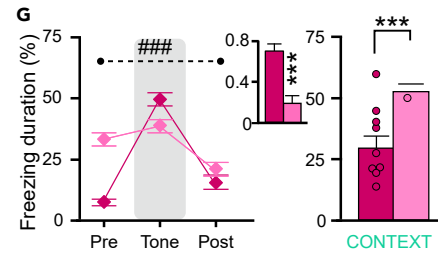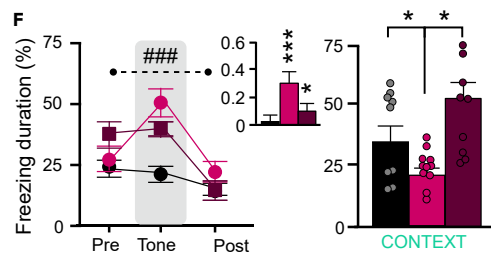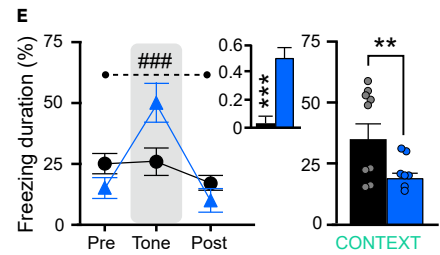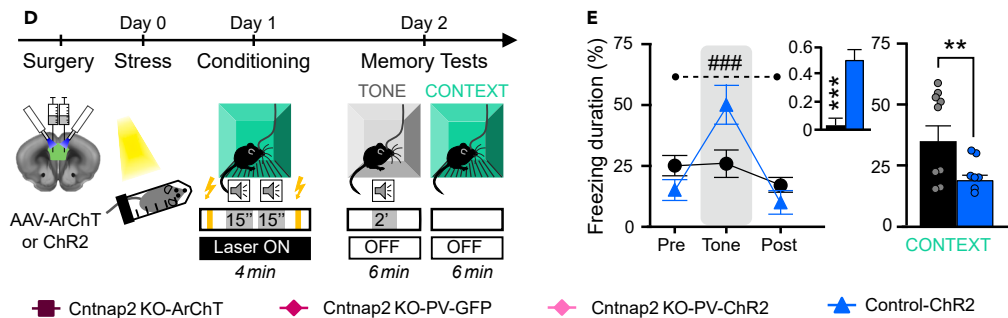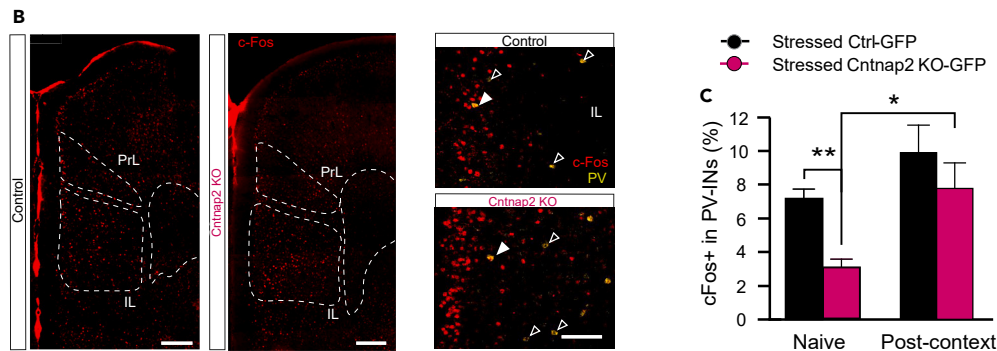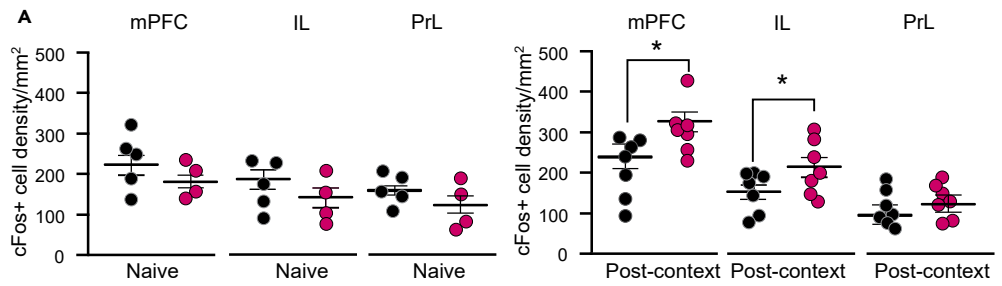
Figure 3. mPFC and PV-INs in the formation of PTSD-like memory

(A) Total naive (left, ns) and context recall-induced c-Fos hyperactivation (right) in the medial pre-frontal cortex (mPFC; Number of cFos+ cells/mm^2; $p < 0.05$), infralimbic (IL; $p < 0.05$), and prelimbic cortex (PrL; ns); Naive: $n = 5$ Control and 4 *Cntnap2* KO mice; trained: $n = 7$ Control and 7 *Cntnap2* KO mice).

(B) Representative images of c-Fos density (red) in the IL and PrL regions of the mPFC (left scale: 250 μm), and specifically in layer 2/3 (right). Plain arrowheads: cFos+ PV+; empty arrowheads: cFos+ PV- cells (10x; scale: 100 μm).

(C) Proportion of cFos positive cells within the PV-INs population, (Naive Control: $n = 5$ vs. Naive *Cntnap2* KO: $n = 5$, $p < 0.01$; Trained Control: $n = 7$; Trained *Cntnap2* KO: $n = 7$, $p < 0.05$).

(D) *In vivo* optogenetics manipulation paradigm.

(E) Fear responses under photostimulation of the pyramidal neurons in ChR2-expressing control mice ($n = 7$; blue) and GFP-infected control mice ($n = 9$; black; tone test; #: significant ChR2 x freezing block repeated measures interaction, $p < 0.001$; tone ratio (inset): $p < 0.001$; context test: $p < 0.01$).

(F) Fear responses under photo-inactivation of the pyramidal neurons in ArChT-infected *Cntnap2* KO mice compared to GFP infected control and *Cntnap2* KO mice (*Cntnap2* KO ArChT: dark red, $n = 9$; *Cntnap2* KO GFP: magenta, $n = 11$, Control GFP: black, $n = 9$; tone test; #: significant ArChT x genotype x freezing block repeated measures interaction, $p < 0.001$; Pre-Tone, KO-GFP vs. ArChT: ns; tone ratio (inset): $p < 0.001$, Control GFP vs. KO-GFP: $p < 0.001$; KO-GFP vs. KO-ArChT: $p < 0.05$; context test (right): control GFP vs. KO-GFP: $p < 0.05$; KO- GFP vs. KO-ArChT: $p < 0.05$).

(G) Fear responses under photostimulation of the parvalbumin interneurons (PV-INs) in ChR2-PV-Cre:*Cntnap2* KO mice compared to GFP-PV-Cre:*Cntnap2* KO mice (ChR2: light pink; $n = 9$; GFP: magenta; $n = 9$; tone test; #: significant ChR2 x freezing block repeated measures interaction, $p < 0.001$; tone ratio (inset): $p < 0.001$; context test: $p < 0.001$).

(H) Social preference tests before and after PTSD protocol (FC) with PV-IN photostimulation during conditioning (STAR methods): % of time interacting with either an unfamiliar mouse or novel object ($n = 7$ GFP; $n = 7$ ChR2; #: experimental group x repeated measures (sessions), $p < 0.001$); Inset: ratio of mouse interaction before and after PTSD protocol (Fear condition (FC); #: Experimental group x repeated measure (sessions) $p < 0.001$).

(I) Total interaction time (%) with both the unfamiliar mouse and the object (ns).

(J) Time spent digging before and after modified PTSD protocol with PV-IN photostimulation during conditioning (STAR methods) ($n = 7$ GFP; $n = 7$ ChR2; Controls vs. KO: $p < 0.0001$). Data are presented as mean ± SEM. ***: $p < 0.001$; **: $p < 0.01$; *: $p < 0.05$; #: interaction significance between repeated measures and genotype. See also Figure S4. See table for precise statistics.

Stress-induced PV-INs alterations

Since an alteration of the excitation/inhibition balance coming from parvalbumin interneuron (PV-INs) hypofunction has been well documented in ASD,[18,30] we then wondered whether PV interneuron activity underpins the observed mPFC hyperactivation and subsequent PTSD-like memory formation. We hypothesized that increasing interneuron activity would prevent traumatic memory formation. We performed optogenetic stimulation of PV-INs via cre-dependent ChR2 activation during conditioning in stressed *Cntnap2* KO mice and found that both PTSD-like memory formation (Figures 3G and S4F–S4I), and the subsequent aggravation of core autistic traits were prevented (Figures 3H–3J).

We next explored the physiological mechanisms priming infralimbic cortex PV-INs to be vulnerable to stress, using *in vitro* electrophysiological recordings in *PV-Cre*; *Td-Tomato* (controls) and *Cntnap2*$^{-/-}$; *PV-Cre*; *Td-Tomato* (KO) mice. As previously reported,[31,32] PV cell number was unchanged between control and KO conditions (Figures S5A–S5C) as were intrinsic properties, such as resting membrane potential and input resistance (Table 1). However, we observed substantial changes in PV-IN firing pattern after stress in control mice, compared to non-stressed control mice (Figure 4, gray and black). As previously described,[33] stress enhances PV-IN excitability in control condition (i.e., reduction in spike latency and increase in maximum firing frequency (Figures 4A–4H and S5D–S5F). Interestingly, our data show that *Cntnap2* KO PV-IN firing resembles that of stressed control PV-INs (Figure 4B, black and light pink). PV-INs in the stressed *Cntnap2* KO condition presented a shift in excitability, characterized by a large increase in latency to first spike (Figures 4C–4E, S5D, and S5E) and a significant decrease in firing frequency at intermediate depolarizing steps, compared to non-stressed KO and control conditions (Figure 4F). This suggests that PV-INs in the *Cntnap2* KO mice compute cortical information following stress differently from the control. These cells are likely to filter more efficiently a certain range of inputs, underlying a global weaker inhibitory power within the mPFC.

These cellular alterations were associated with changes in the expression of activity-dependent proteins that fine-tune PV-IN firing, i.e., the calcium/calmodulin-dependent Etv1/Er81 transcription factor, which regulates PV-IN spike latency at near threshold potential,[34] and the calcium-binding protein parvalbumin (PV;[35]), which expression levels depend on cell activity.[36] In line with the shifted firing latency (Dehorter et al.,[34]; Figures 4C–4E), we found decreased Etv1/Er81 levels in control PV-INs upon stress (Figures 4I and 4J top panel) but increased Etv1/Er81 expression in the *Cntnap2* KO condition after stress, compared to non-stressed condition.

As previously reported,[31] PV levels were significantly decreased between control and *Cntnap2* KO conditions (Figures 4I and 4J bottom panel; Figure S5C). While no change was observed upon stress in control, PV expression significantly increased in stressed *Cntnap2* KO mice, compared to non-stressed mice (Figures 4I and 4J bottom panel; Figure S5C). At the synaptic level, stress did not affect spontaneous inputs (Figures S5G and S5H) and release probability onto PV-INs (Figures 4K, 4L, S5I, and S5J) in control and *Cntnap2* KO conditions. However, the amplitude of the evoked inputs afferent to PV-INs was increased upon stress in control (Figure 4M, black). This was not the case for the *Cntnap2* KO condition (Figure 4M, pink), suggesting that stress elicits differential regulation of the evoked inputs afferent to PV-INs. Overall, these data indicate that PV-INs in the *Cntnap2* KO mice display similar properties to stressed PV-INs in the control condition and also present with an altered adaptation to stress that is likely to underlie a deficit in inhibition in the infralimbic cortex of mPFC.

DISCUSSION

Overall, this work uncovers a reciprocal relationship between PTSD-like memory formation and the core traits of ASD. While deficits in stress processing are well-known in ASD, there has been a lack of research into the risk of PTSD development in autism that stems from a poor

Table 1. Electrophysiological properties of the parvalbumin interneurons of the prefrontal cortex in non-stressed and stressed control and Cntnap2 KO mice

	Control		*Cntnap2* KO		
	Non-stressed	Stressed	Non-stressed	Stressed	*p*-values
Vrest (mV)	-65.63 ± 1.81	-65.89 ± 1.47	-71.96 ± 1.10	-66.91 ± 1.69	Stress × Genotype: $p = 0.1201$; Non-stress Ctrl vs. non-Stressed Cntnap2 KO: $p = 0.0151$
Rm (MΩ)	152.78 ± 2.49	156.32 ± 1.70	152.67 ± 2.10	154.80 ± 1.09	Stress × Genotype: $p = 0.4413$; Non-stress Ctrl vs. non-Stressed Cntnap2 KO: $p = 0.7256$; Stress in Controls: $p = 0.0724$; Stress in Cntnap2 KO: $p = 0.5928$
V threshold (mV)	-34.42 ± 1.66	-33.38 ± 1.61	-33.20 ± 3.85	-34.86 ± 1.61	Stress × Genotype: $p = 0.4929$; Non-stress Ctrl vs. non-Stressed Cntnap2 KO: $p = 0.6342$; Stress in Controls: $p = 0.6323$; Stress in Cntnap2 KO: $p = 0.6253$
AP amplitude (mV)	39.50 ± 3.550	34.75 ± 1.767	33.80 ± 2.390	27.01 ± 4.718	Stress × Genotype: $p = 0.8904$; Non-stress Ctrl vs. non-Stressed Cntnap2 KO: $p = 0.1560$; Stress in Controls: $p = 0.2145$; Stress in Cntnap2 KO: $p = 0.2579$
AP rise time 10–90% (ms)	0.50 ± 0.07	0.61 ± 0.18	0.37 ± 0.05	0.34 ± 0.02	Stress x Genotype: $p = 0.5415$; Non-stress Ctrl vs. non-Stressed Cntnap2 KO: $p = 0.1841$; Stress in Controls: $p = 0.6258$; Stress in Cntnap2 KO: $p = 0.5111$
AP half-width (ms)	0.79 ± 0.11	0.64 ± 0.04	0.61 ± 0.04	0.60 ± 0.03	Stress × Genotype: $p = 0.4771$; Non-stress Ctrl vs. non-Stressed Cntnap2 KO: $p = 0.1793$; Stress in Controls: $p = 0.1596$; Stress in Cntnap2 KO: $p = 0.4166$
AP Decay 90-10% (ms)	0.58 ± 0.07	0.52 ± 0.05	0.50 ± 0.05	0.51 ± 0.05	Stress × Genotype: $p = 0.9048$; Non-stress Ctrl vs. non-Stressed Cntnap2 KO: $p = 0.7658$; Stress in Controls: $p = 0.5185$; Stress in Cntnap2 KO: $p = 0.4488$
AHP peak (mV)	-13.09 ± 1.33	-12.08 ± 1.24	-14.30 ± 1.19	-14.55 ± 2.35	Stress × Genotype: $p = 0.4563$; Non-stress Ctrl vs. non-Stressed Cntnap2 KO: $p = 0.4949$; Stress in Controls: $p = 0.6080$; Stress in Cntnap2 KO: $p = 0.5948$

Non-stressed PV-Cre; td-Tomato: $n = 7$ cells, 4 mice; Stressed PV-Cre; td-Tomato: $n = 9$ cells, 4 mice; Non-stressed *Cntnap2*$^{-/-}$; PV-Cre; td-Tomato: $n = 10$ cells, 5 mice; Stressed *Cntnap2*$^{-/-}$; PV-Cre; td-Tomato: $n = 8$ cells, 4 mice. 2-way ANOVA: $*p < 0.05$.

understanding of the combined disorders and the absence of suitable detection tools.[9,37,38] Here, we demonstrate in four mouse models of ASD that pre-exposure to a single stress is sufficient to result in the PTSD-like memory of a subsequent stressful experience, contrary to a control population.[1] This study therefore provides the first direct demonstration that ASD is associated with a risk of developing PTSD-like memory for mildly stressful situations. It corroborates with the hypotheses of clinicians positing that vulnerable populations could develop PTSD for levels of stress that are not "extreme" as defined by the DSM5.[8]

The susceptibility to produce traumatic memory from non-traumatic paradigm in the ASD models likely occurs due to a cumulative effect of stressful stimuli. This concept has been previously explored with the "3-hit" stress model[39] and the stress-enhanced fear learning (SEFL) rodent paradigm.[40] In the context of this study, mice that underwent the classic PTSD paradigm can be considered to undergo a traumatic episode consisting of two sequential adverse events (Fear conditioning followed by restraint stress). Conversely, mice that underwent the modified PTSD paradigm can be considered to undergo a non-traumatic episode (restraint stress followed by fear conditioning 24 h later). As ASD mice models displayed intact contextual memory capacities in non-stressful situations, we suggest that an impaired ability to cope with stressful situations is responsible for the switch from normal to PTSD-like memory. Therefore, genotype itself can be considered the first hit, and the pre-exposure to stress the second hit, the fear conditioning session being the third hit.

Human functional imaging and animal model studies suggest that cortical circuit abnormalities in ASD contribute to altered sensory representations and difficulties in stress coping. Our analysis uncovers the specific circuit alterations underlying the hypersensitivity to stress that leads to PTSD-like memory formation in ASD and allows the reinterpretation of the role of the circuitry responsible for PTSD-like memory formation in general. PTSD is indeed thought to be driven by amygdala hyperfunctioning, underlying the observed excessive fear. Yet, we
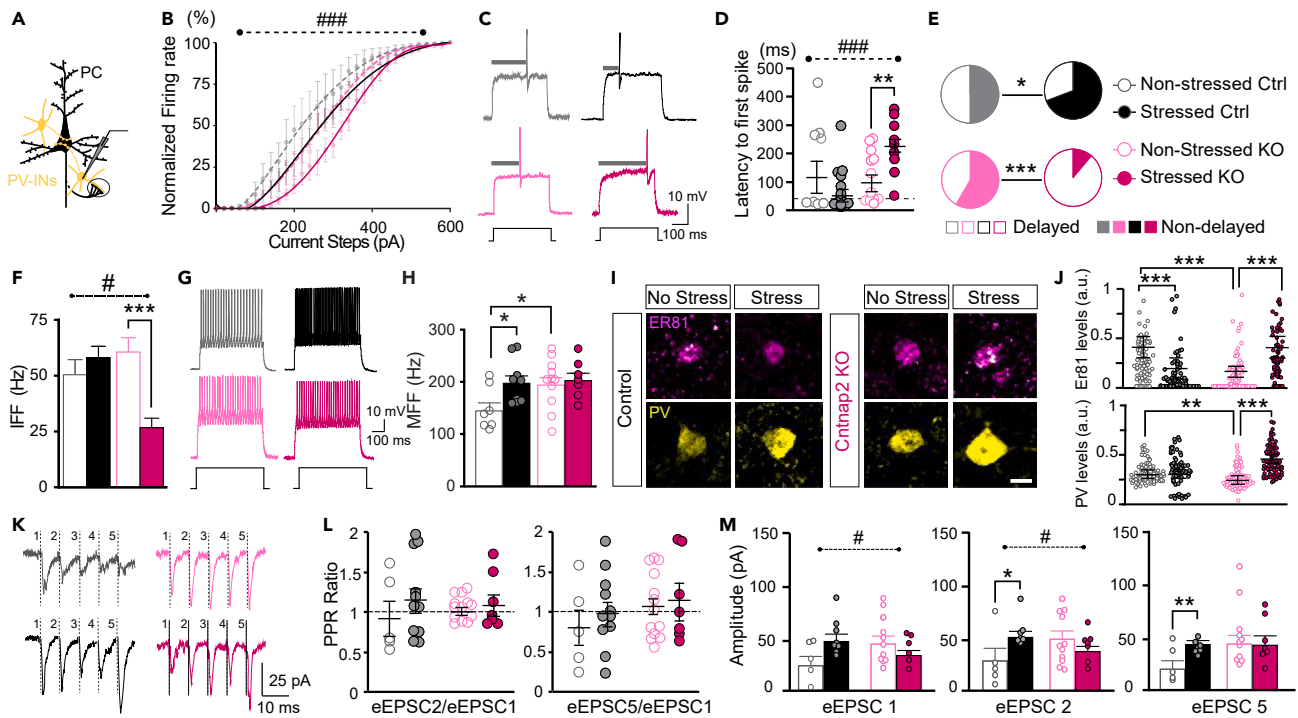
Figure 4. Effect of stress on PV-INs in controls and *Cntnap2* KO

(A) Schematics of the *in vitro* electrophysiological recording of PV-INs in the mPFC; PC: pyramidal cell.

(B) Normalized PV-IN firing rate (% of maximum firing frequency) as a function of injected current steps (#: evolution of spike frequency x stress: *p* < 0.001) for non-stressed controls (light gray; *n* = 7), stressed controls (black; *n* = 9), non-stressed *Cntnap2* KO (light pink; *n* = 11), and stressed *Cntnap2* KO (dark pink; *n* = 7) conditions.

(C) Representative traces of PV-IN firing at threshold potential.

(D) Latency to first spike (#: Interaction stress x genotype: *p* < 0.001; stress in controls: ns; stress in *Cntnap2* KO: *p* < 0.01). Dashed line represents limit (see STAR methods) between delayed vs. non-delayed cells.

(E) Proportion of delayed vs. non-delayed PV-INs in non-stressed and stressed conditions in control (Chi square test: *p* < 0.05) and *Cntnap2* KO mice (*p* < 0.001).

(F) Mean firing frequency at intermediate steps (IFF; 100–400 pA; #: stress x genotype: *p* < 0.05; stress in controls: ns; stress in *Cntnap2* KO: *p* < 0.001).

(G) Representative traces of PV-IN firing at maximum firing frequency (MFF, 600 pA).

(H) MFF at 600 pA (stress in controls: *p* < 0.05; non-stressed control vs. non-stressed KO: *p* < 0.05).

(I) Representative illustrations of the expression of Er81 (magenta) and PV (yellow) in each experimental group (scale: 10 μm).

(J) Mean Er81 (top) and PV (bottom) expression levels (a.u.: arbitrary unit; Er81: stress in controls: *p* < 0.001; stress in *Cntnap2* KO: *p* < 0.001; Genotype in non-stressed: *p* < 0.001; PV: stress in controls: ns; stress in *Cntnap2* KO: *p* < 0. 001; Genotype in non-stressed: *p* < 0.01). Non-stressed Control *n* = 4 mice, 82 cells; Control stressed *n* = 4 mice, 69 cells; non-stressed Cntnap2 KO *n* = 4 mice, 78 cells; Stressed Cntnap2 KO *n* = 5 mice, 80 cells.

(K) Representative traces of 40 Hz paired-pulse ratios (PPR).

(L) PPR ratio between 1st and 2nd evoked excitatory postsynaptic currents (eEPSC, left) and 1st and 5th EPSCs (right); *n* = 5 no stress control; *n* = 8 stressed control; *n* = 11 *Cntnap2* KO no stress; *n* = 7 *Cntnap2* KO stress; ns for both.

(M) Mean eEPSC amplitude (pA); #: interaction stress x genotype: *p* < 0.05, *p* < 0.05, and ns for EPSC1, EPSC2 and EPSC5, respectively; stress in control: ns, *p* < 0.05 and *p* < 0.01; stress in *Cntnap2* KO: ns, ns, ns. Data are presented as mean ± SEM. ***: *p* < 0.001; **: *p* < 0.01; *: *p* < 0.05. from two-way ANOVA; see table for precise statistics. See also Figure S5 and Table 1.

observed the development of PTSD-like memory, associated with hypoactivation of the amygdala in the *Cntnap2 KO* mice. Interestingly, we also found hippocampus hypoactivation, likely underlying contextual amnesia.[22] Together, our results confirm the involvement of the hippocampus and contextualization in determining the nature of the memory formed during a stressful event in both ASD and PTSD. This work also calls for reevaluating the mechanisms underlying traumatic memory formation, which can be triggered by IL hyperactivation during trauma, combined with a (non-traumatic) acute stress in ASD mouse models (Figures 1 and 3), and not by mPFC hypoactivation, as currently established for PTSD.[14,41] We therefore provide new grounds to further dissect PTSD and its overlap with ASD pathophysiology. It would be interesting to include in future investigations specific analysis and manipulation not only of the subregions of the PFC (i.e., infralimbic vs. prelimbic) but also of hippocampus (i.e., CA1 vs. CA3 vs. DG) and amygdala (i.e., basolateral, lateral vs. central), since these distinct areas present anatomical and functional differences that may be relevant to specific memory functions in autism.

By revealing how cell input-output function is modulated in the *Cntnap2* KO mouse model of ASD, with the homeostatic capabilities of cortical interneurons altered after stress, we show that the PV-INs of the mPFC are directly responsible for traumatic memory formation in a

model of ASD. In response to stress, PV-INs in the control condition are more excitable (i.e., decreased latency to first spike, increased firing frequency; Figure 4), increasing their inhibitory power. This is a necessary adaptive response, mediating the fine-tuned activation of the mPFC during stress.[42] However, PV-INs in the *Cntnap2* KO condition do not display this adaptive response, instead showing decreased excitability following stress (i.e., increased latency to first spike, decreased firing frequency; Figure 4), and thus a lower inhibitory power within the circuit.[34,43] These deficits therefore underlie IL hyperactivation, preventing the *Cntnap2* KO mice from adapting adequately to stress, and in turn leading to PTSD-like memory formation (Graphical abstract). It would be of interest to confirm the PV-IN vulnerability in different models of ASD and to further describe the role of PV-INs in PTSD, as this investigation has been limited,[44–46] and could uncover additional convergent mechanisms for ASD and PTSD centering around this interneuron population. In addition, PV-INs pose as potential targets for therapeutic intervention as they have been shown to restore balance in the mPFC circuit.[18] Modulating the activity of the PV-INs in mice models of ASD would be an insightful investigation to restore normal memory and reduce the core symptoms of ASD.

Overall, our study provides a new tool to further dissect the overlap between PTSD and ASD and the underlying alterations in emotional memory. It encourages future research to investigate the crucial role of the PV-INs in enhanced stress-sensitivity and maladaptive fear memory in ASD, and the implication of other interneurons, such as somatostatin-positive cells, that may also contribute.

The recontextualization therapeutic approach reveals that pathological memory can be reshaped into adapted fear memory. By reactivating the traumatic memory in the original environment, recontextualization allows the re-allocation of trauma representation into specific context, thereby suppressing abnormal hypermnesia.[22] Remarkably, normalizing PTSD-like memory also induced a reduction in the intensity of the autistic traits. While the precise mechanisms remain to be described, the activity of the hippocampus was previously shown to be critical during recontextualization.[22] It is therefore possible that hippocampal activation has a beneficial effect upon the autistic traits, especially social behaviors.[47]

Behaviorally, ASD and PTSD display similar characteristics,[26] including impaired emotional regulation, cognitive rigidity, and fragmented autobiographical memory.[5] Our study overall describes a reciprocal relationship between the PTSD-like memory formation and the autistic traits. One can speculate that addressing potential undiagnosed traumatic memories in autistic people could alleviate some of the most challenging aspects of the autistic presentation. While this is promising, one caveat for the implementation of this procedure in patients will arise from being able to identify the origin of the trauma and detect PTSD in ASD. Our results suggest that everyday life situations could be experienced as traumatic in ASD patients, as previously suggested in clinical studies.[8,48] As new methods of detection emerge,[49] our study calls for better use of predictive tools that enable efficient risk assessment and early interventions of PTSD among those likely to experience trauma, such as people with autism. Timely detection appears essential since PTSD worsens the core ASD traits and is strongly associated with various psychiatric comorbidities and suicide.[50]

Limitations of the study

PTSD presentation is complex and consists in re-experiencing a threatening event in the form of persistent and intrusive memories (i.e., traumatic memory), avoidance of reminders of the event, and emotional numbing.[1] However, clinicians consider the unusual nature of the traumatic memory as the prominent feature of PTSD, characterized by both involuntary hypermnesia for some isolated trauma-related stimuli and declarative amnesia for surrounding context.[51,52] This maladaptive memory profile is reflected in the paradigms used in this study. In our conditions, this consists of excessive freezing in mice during the tone test (i.e., a salient traumatic cue) and low freezing in the traumatic context. Currently, no perfect model for PTSD exists as there are several characteristics that are specific to humans. However, the originality of the approach used in this study lies in the analysis of the qualitative alterations specific to PTSD-like memory observed in patients by clinicians, i.e., hypermnesia/amnesia profile.[51,52] Future investigations should aim to further study other important aspects of PTSD that are relevant to human behavior, such as anxiety and emotional numbing.[1]

Finally, while differences in rearing conditions of non-littermates *Cntnap2* control and KO mice may have influenced stress coping, they do not alone generate the phenotype, as the other genetic mouse models of ASD (i.e., littermates Shank3 KO, Pten cKO, and Fmr1 KO) presented PTSD-like memory formation upon similar paradigm.

STAR★METHODS

Detailed methods are provided in the online version of this paper and include the following:

- KEY RESOURCES TABLE
- RESOURCE AVAILABILITY
  - Lead contact
  - Materials availability
  - Data and code availability
- EXPERIMENTAL MODEL AND STUDY PARTICIPANT DETAILS
- METHOD DETAILS
  - Fear conditioning procedure
  - Assessment of the persistence of PTSD-like fear memory
  - Assessment of the core symptoms of ASD
  - Optogenetic manipulation of the mPFC

- ○ Immunohistochemistry
- ○ *In vitro* electrophysiology
- ● QUANTIFICATION AND STATISTICAL ANALYSIS

SUPPLEMENTAL INFORMATION

Supplemental information can be found online at https://doi.org/10.1016/j.isci.2024.109747.

AUTHOR CONTRIBUTIONS

Conceptualization: N.D. and A.S.A.; methodology: N.D., A.S.A., and A.D.; investigation: A.S.A., T.V.A., Y.S., A.S., N.Y.A., and E.C.R.; supervision: N.D. and A.S.A.; writing – original draft: N.D. and A.S.A.; writing – review and editing: N.D., A.S.A., N.Y.A., A.M., and A.D.

DECLARATION OF INTERESTS

The authors declare no competing interests.

REFERENCES

1. DSM-5, and Association American Psychiatric (2013). Diagnostic and Statistical Manual of Mental Disorders : DSM-5.
2. Möhrle, D., Fernández, M., Peñagarikano, O., Frick, A., Allman, B., and Schmid, S. (2020). What we can learn from a genetic rodent model about autism. Neurosci. Biobehav. Rev. *109*, 29–53. https://doi.org/10.1016/j.neubiorev.2019.12.015.
3. Lyall, K., Schweitzer, J.B., Schmidt, R.J., Hertz-Picciotto, I., and Solomon, M. (2017). Inattention and Hyperactivity in Association With Autism Spectrum Disorders in the CHARGE Study. Res. Autism Spectr. Disord. *35*, 1–12. https://doi.org/10.1016/J.RASD.2016.11.011.
4. Markram, K., Rinaldi, T., La Mendola, D., Sandi, C., and Markram, H. (2008). Abnormal fear conditioning and amygdala processing in an animal model of autism. Neuropsychopharmacology *33*, 901–912. https://doi.org/10.1038/sj.npp.1301453.
5. Solomon, M., Mccauley, J.B., Iosif, A.M., Carter, C.S., and Ragland, J.D. (2016). Cognitive control and episodic memory in adolescents with autism spectrum disorders. Neuropsychologia *89*, 31–41. https://doi.org/10.1016/j.neuropsychologia.2016.05.013.
6. Desmedt, A., Marighetto, A., and Piazza, P.-V. (2015). Abnormal Fear Memory as a Model for Posttraumatic Stress Disorder. Biol. Psychiatry *78*, 290–297. https://doi.org/10.1016/J.BIOPSYCH.2015.06.017.
7. Haruvi-Lamdan, N., Horesh, D., Zohar, S., Kraus, M., and Golan, O. (2020). Autism Spectrum Disorder and Post-Traumatic Stress Disorder: An unexplored co-occurrence of conditions. Autism *24*, 884–898. https://doi.org/10.1177/1362361320912143.
8. Brewin, C.R., Rumball, F., and Happé, F. (2019). Neglected causes of post-traumatic stress disorder. BMJ *365*, l2372. https://doi.org/10.1136/bmj.l2372.
9. Rumball, F. (2019). A Systematic Review of the Assessment and Treatment of Posttraumatic Stress Disorder in Individuals with Autism Spectrum Disorders. Rev. J. Autism Dev. Dis.) *6*, 294–324.
10. Tovote, P., Fadok, J.P., and Lüthi, A. (2015). Neuronal circuits for fear and anxiety. Nat. Rev. Neurosci. *16*, 317–331. https://doi.org/10.1038/nrn3945.
11. Courtin, J., Chaudun, F., Rozeske, R.R., Karalis, N., Gonzalez-Campo, C., Wurtz, H., Abdi, A., Baufreton, J., Bienvenu, T.C.M., and Herry, C. (2014). Prefrontal parvalbumin interneurons shape neuronal activity to drive fear expression. Nature *505*, 92–96. https://doi.org/10.1038/nature12755.
12. Al Abed, A.S., Sellami, A., Brayda-Bruno, L., Lamothe, V., Noguès, X., Potier, M., Bennetau-Pelissero, C., and Marighetto, A. (2016). Estradiol enhances retention but not organization of hippocampus-dependent memory in intact male mice. Psychoneuroendocrinology *69*, 77–89. https://doi.org/10.1016/j.psyneuen.2016.03.014.
13. Lazaro, M.T., Taxidis, J., Shuman, T., Bachmutsky, I., Ikrar, T., Santos, R., Marcello, G.M., Mylavarapu, A., Chandra, S., Foreman, A., et al. (2019). Reduced Prefrontal Synaptic Connectivity and Disturbed Oscillatory Population Dynamics in the CNTNAP2 Model of Autism. Cell Rep. *27*, 2567–2578.e6. https://doi.org/10.1016/j.celrep.2019.05.006.
14. Alexandra Kredlow, M., Fenster, R.J., Laurent, E.S., Ressler, K.J., and Phelps, E.A. (2022). Prefrontal cortex, amygdala, and threat processing: implications for PTSD. Neuropsychopharmacology *47*, 247–259. https://doi.org/10.1038/s41386-021-01155-7.
15. Yizhar, O., Fenno, L.E., Prigge, M., Schneider, F., Davidson, T.J., O'Shea, D.J., Sohal, V.S., Goshen, I., Finkelstein, J., Paz, J.T., et al. (2011). Neocortical excitation/inhibition balance in information processing and social dysfunction. Nature *477*, 171–178. https://doi.org/10.1038/nature10360.
16. Chen, C.C., Lu, J., Yang, R., Ding, J.B., and Zuo, Y. (2018). Selective activation of parvalbumin interneurons prevents stress-induced synapse loss and perceptual defects. Mol. Psychiatry *23*, 1614–1625. https://doi.org/10.1038/mp.2017.159.
17. Antoine, M.W., Langberg, T., Schnepel, P., Feldman, D.E., and Biology, C. (2019). Circuit Excitability in Four Autism Mouse Models. Neuron *101*, 648–661.e4. https://doi.org/10.1016/j.neuron.2018.12.026. Increased.
18. Selimbeyoglu, A., Kim, C.K., Inoue, M., Lee, S.Y., Hong, A.S.O., Kauvar, I., Ramakrishnan, C., Fenno, L.E., Davidson, T.J., Wright, M., and Deisseroth, K. (2017). Modulation of prefrontal cortex excitation/inhibition balance rescues social behavior in CNTNAP2-deficient mice. Sci. Transl. Med. *9*, eaah6733. https://doi.org/10.1126/scitranslmed.aah6733.
19. Peñagarikano, O., and Geschwind, D.H. (2012). What does CNTNAP2 reveal about autism spectrum disorder? Trends Mol. Med.

18, 156–163. https://doi.org/10.1016/j. molmed.2012.01.003.

20. Brewin, C.R. (2011). The Nature and Significance of Memory Disturbance in Posttraumatic Stress Disorder. Annu. Rev. Clin. Psychol. *7*, 203–227. https://doi.org/10. 1146/ANNUREV-CLINPSY-032210-104544.

21. Kaouane, N., Porte, Y., Vallée, M., Brayda-Bruno, L., Mons, N., Calandreau, L., Marighetto, A., Piazza, P.V., and Desmedt, A. (2012). Glucocorticoids can induce PTSD-like memory impairments in mice. Science *335*, 1510–1513. https://doi.org/10.1126/science. 1207615.

22. Al Abed, A.S., Ducourneau, E.-G., Bouarab, C., Sellami, A., Marighetto, A., and Desmedt, A. (2020). Preventing and treating PTSD-like memory by trauma contextualization. Nat. Commun. *11*, 4220–4229. https://doi.org/10. 1038/s41467-020-18002-w.

23. Brewin, C.R., Gregory, J.D., Lipton, M., and Burgess, N. (2010). Intrusive Images in Psychological Disorders: Characteristics, Neural Mechanisms, and Treatment Implications. Psychol. Rev. *117*, 210–232. https://doi.org/10.1037/ a0018113.

24. Rademacher, S., and Eickholt, B.J. (2019). PTEN in Autism and Neurodevelopmental Disorders. Cold Spring Harb. Perspect. Med. *9*, a036780. https://doi.org/10.1101/ cshperspect.a036780.

25. Aloisi, E., Le Corf, K., Dupuis, J., Zhang, P., Ginger, M., Labrousse, V., Spatuzza, M., Georg Haberl, M., Costa, L., Shigemoto, R., et al. (2017). Altered surface mGluR5 dynamics provoke synaptic NMDAR dysfunction and cognitive defects in Fmr1 knockout mice. Nat. Commun. *8*, 1103. https://doi.org/10.1038/s41467-017-01191-2.

26. Haruvi-lamdan, N., Horesh, D., and Golan, O. (2018). PTSD and Autism Spectrum Disorder : Co-morbidity , Gaps in Research and Potential Shared Mechanisms PTSD and Autism Spectrum Disorder : Co-morbidity , Gaps in Research and Potential Shared Mechanisms. Psychol. Trauma. *10*, 290–299. https://doi.org/10.1037/ tra0000298.

27. Ressler, R.L., Goode, T.D., Kim, S., Ramanathan, K.R., and Maren, S. (2021). Covert capture and attenuation of a hippocampus-dependent fear memory. Nat. Neurosci. *24*, 677–684. https://doi.org/10. 1038/s41593-021-00825-5.

28. Fenster, R.J., Lebois, L.A.M., Ressler, K.J., and Suh, J. (2018). Brain circuit dysfunction in traumatic stress disorder : from mouse to man. Nat. Rev. Neurosci. *19*, 535–551. https://doi.org/10.1038/ s41583-018-0039-7.

29. Dahlgren, M.K., Laifer, L.M., VanElzakker, M.B., Offringa, R., Hughes, K.C., Staples-Bradley, L.K., Dubois, S.J., Lasko, N.B., Hinojosa, C.A., Orr, S.P., et al. (2018). Diminished medial prefrontal cortex activation during the recollection of stressful events is an acquired characteristic of PTSD. Psychol. Med. *48*, 1128–1138. https://doi.org/10.1017/ S003329171700263X.

30. Filice, F., Janickova, L., Henzi, T., Bilella, A., and Schwaller, B. (2020). The Parvalbumin Hypothesis of Autism Spectrum Disorder. Front. Cell. Neurosci. *14*, 577525. https:// doi.org/10.3389/FNCEL.2020.577525/ BIBTEX.

31. Scott, R., Sánchez-Aguilera, A., Van Elst, K., Lim, L., Dehorter, N., Bae, S.E., Bartolini, G., Peles, E., Kas, M.J.H., Bruining, H., and Marín, O. (2019). Loss of Cntnap2 Causes Axonal Excitability Deficits, Developmental Delay in Cortical Myelination, and Abnormal Stereotyped Motor Behavior. Cereb. Cortex *29*, 586–597. https://doi.org/10.1093/cercor/ bhx341.

32. Antoine, M.W., Langberg, T., Schnepel, P., and Feldman, D.E. (2019). Increased Excitation-Inhibition Ratio Stabilizes Synapse and Circuit Excitability in Four Autism Mouse Models. Neuron *101*, 648–661.e4. https://doi.org/10.1016/J. NEURON.2018.12.026/ATTACHMENT/ F67EFB49-A775-4AFF-91DC-EAE949675912/MMC1.PDF.

33. Page, C.E., Shepard, R., Heslin, K., and Coutellier, L. (2019). Prefrontal parvalbumin cells are sensitive to stress and mediate anxiety-related behaviors in female mice. Sci. Rep. 19772. https://doi.org/10.1038/s41598-019-56424-9.

34. Dehorter, N., Ciceri, G., Bartolini, G., Lim, L., del Pino, I., and Marín, O. (2015). Tuning of fast-spiking interneuron properties by an activity-dependent transcriptional switch. Science *349*, 1216–1220. https://doi.org/10. 1126/science.aab3415.

35. Lauber, E., Filice, F., and Schwaller, B. (2018). Dysregulation of Parvalbumin Expression in the Cntnap2−/− Mouse Model of Autism Spectrum Disorder. Front. Mol. Neurosci. *11*, 262. https://doi.org/10.3389/fnmol.2018. 00262.

36. Donato, F., Rompani, S.B., and Caroni, P. (2013). Parvalbumin-expressing basket-cell network plasticity induced by experience regulates adult learning. Nature *504*, 272–276. https://doi.org/10.1038/ nature12866.

37. Fuld, S. (2018). Autism Spectrum Disorder: The Impact of Stressful and Traumatic Life Events and Implications for Clinical Practice. Clin. Soc. Work. J. *46*, 210–219. https://doi. org/10.1007/S10615-018-0649-6.

38. Rumball, F., Brook, L., Happé, F., and Karl, A. (2021). Heightened risk of posttraumatic stress disorder in adults with autism spectrum disorder: The role of cumulative trauma and memory deficits. Res. Dev. Disabil. *110*, 103848. https://doi.org/10.1016/J.RIDD. 2020.103848.

39. Daskalakis, N.P., Bagot, R.C., Parker, K.J., Vinkers, C.H., and de Kloet, E.R. (2013). The three-hit concept of vulnerability and resilience: Toward understanding adaptation to early-life adversity outcome. Psychoneuroendocrinology *38*, 1858–1873. https://doi.org/10.1016/J.PSYNEUEN.2013. 06.008.

40. Nishimura, K.J., Poulos, A.M., Drew, M.R., and Rajbhandari, A.K. (2022). Know thy SEFL: Fear sensitization and its relevance to stressor-related disorders. Neurosci. Biobehav. Rev. *142*, 104884. https://doi. org/10.1016/J.NEUBIOREV.2022.104884.

41. Elzinga, B.M., and Bremner, J.D. (2002). Are the neural substrates of memory the final common pathway in posttraumatic stress disorder (PTSD)? J. Affect. Disord. *70*, 1–17. https://doi.org/10.1016/S0165-0327(01) 00351-2.

42. Jacobs, D.S., and Moghaddam, B. (2021). Medial prefrontal cortex encoding of stress and anxiety. Int. Rev. Neurobiol. *158*, 29–55. https://doi.org/10.1016/bs.irn.2020.11.014.

43. Golomb, D., Donner, K., Shacham, L., Shlosberg, D., Amitai, Y., and Hansel, D. (2007). Mechanisms of Firing Patterns in Fast-Spiking Cortical Interneurons. PLoS Comput. Biol. *3*, e156. https://doi.org/10.1371/ JOURNAL.PCBI.0030156.

44. Sun, X.R., Zhang, H., Zhao, H.T., Ji, M.H., Li, H.H., Wu, J., Li, K.Y., and Yang, J.J. (2016). Amelioration of oxidative stress-induced phenotype loss of parvalbumin interneurons might contribute to the beneficial effects of environmental enrichment in a rat model of post-traumatic stress disorder. Behav. Brain Res. *312*, 84–92. https://doi.org/10.1016/J. BBR.2016.06.016.

45. Binette, A.N., Liu, J., Bayer, H., Crayton, K.L., Melissari, L., Sweck, S.O., and Maren, S. (2023). Parvalbumin-Positive Interneurons in the Medial Prefrontal Cortex Regulate Stress-Induced Fear Extinction Impairments in Male and Female Rats. J. Neurosci. *43*, 4162–4173. https://doi.org/10.1523/JNEUROSCI.1442-22.2023.

46. Chen, Y.H., Lan, Y.J., Zhang, S.R., Li, W.P., Luo, Z.Y., Lin, S., Zhuang, J.P., Li, X.W., Li, S.J., Yang, J.M., and Gao, T.M. (2017). ErbB4 signaling in the prelimbic cortex regulates fear expression. Transl. Psychiatry *7*, e1168. https://doi.org/10.1038/tp. 2017.139.

47. Banker, S.M., Gu, X., Schiller, D., and Foss-Feig, J.H. (2021). Hippocampal contributions to social and cognitive deficits in autism spectrum disorder. Trends Neurosci. *44*, 793–807. https://doi.org/10.1016/j.tins.2021. 08.005.

48. Rumball, F., Happé, F., and Grey, N. (2020). Experience of Trauma and PTSD Symptoms in Autistic Adults: Risk of PTSD Development Following DSM-5 and Non-DSM-5 Traumatic Life Events. Autism Res. *13*, 2122–2132. https://doi.org/10.1002/ aur.2306.

49. Papini, S., Norman, S.B., Campbell-Sills, L., Sun, X., Stein, M.B., He, F., Kessler, R.C., Ursano, R.J., and Jain, S. (2023). Development and Validation of a Machine Learning Prediction Model of Posttraumatic Stress Disorder After Military Deployment. JAMA Netw. Open *6*, e2321273. https://doi. org/10.1001/JAMANETWORKOPEN.2023. 21273.

50. Stanley, I.H. (2021). Advancements in the understanding of PTSD and suicide risk: Introduction to a special section. Psychol. Trauma. *13*, 723–724. https://doi.org/10. 1037/TRA0001121.

51. Brewin, C.R. (2007). What is it that a neurobiological model of PTSD must explain? Prog. Brain Res. *167*, 217–228. https://doi.org/10.1016/S0079-6123(07) 67015-0.

52. Van der Kolk, B.A., Hopper, J.W., and Osterman, J.E. (2001). Exploring the nature of traumatic memory: Combining clinical knowledge with laboratory methods. J. Aggr. Maltreat. Trauma *4*, 9–31. https://doi.org/10.1300/ J146v04n02_02.

53. Peñagarikano, O., Abrahams, B.S., Herman, E.I., Winden, K.D., Gdalyahu, A., Dong, H., Sonnenblick, L.I., Gruver, R., Almajano, J., Bragin, A., et al. (2011). Absence of CNTNAP2 leads to epilepsy, neuronal migration abnormalities, and core autism-related deficits. Cell *147*, 235–246. https://doi.org/10.1016/j.cell. 2011.08.040.

54. Brewin, C.R. (2008). What is it that a neurobiological model of PTSD must explain? Prog. Brain Res. *167*, 217–228. https://doi.org/10.1016/S0079-6123(07)67015-0.

55. Fanselow, M.S. (1980). Conditional and unconditional components of post-shock freezing. Pavlov. J. Biol. Sci. *15*, 177–182. https://doi.org/10.1007/BF03001163.

56. van den Boom, B.J.G., Pavlidi, P., Wolf, C.J.H., Mooij, A.H., and Willuhn, I. (2017). Automated classification of self-grooming in mice using open-source software. J. Neurosci. Methods *289*, 48–56. https://doi.org/10.1016/J.JNEUMETH.2017.05.026.

57. Deacon, R.M.J. (2006). Digging and marble burying in mice: simple methods for in vivo identification of biological impacts. Nat. Protoc. *1*, 122–124. https://doi.org/10.1038/nprot.2006.20.

58. Noldus, L.P.J.J., Spink, A.J., and Tegelenbosch, R.A.J. (2001). EthoVision: A versatile video tracking system for automation of behavioral experiments. Behav. Res. Methods Instrum. Comput. *33*, 398–414. https://doi.org/10.3758/BF03195394/METRICS.

STAR★METHODS

KEY RESOURCES TABLE

REAGENT or RESOURCE	SOURCE	IDENTIFIER
Antibodies		
Mouse anti cFos	Santa Cruz	SC166940, RRID:AB_10609634
Goat anti-PV	SWANT	PVG-214, RRID:AB_2313848
rabbit anti-Etv1/Er81	Prof S. Arber	BioZentrum
chicken anti-GFP	Aves Labs	GFP-1020, RRID:AB_10000240
Alexa Fluor® 488 goat anti-chicken IgG (H + L)	Thermo Fisher Scientific	A-11039, RRID:AB_2534096
Goat-488	Molecular Probes	A11055, RRID:AB_2534102
Streptavidin 555	Thermo Fisher Scientific	S21381, RRID:AB_2307336
Mouse-Biotin	Vector Laboratories	BA-2000, RRID:AB_2313581
DAPI	Sigma	D9542-10MG
Bacterial and virus strains		
AAV5-pCaMKIIα-ArchT-GFP	UNC Vector Core	N/A
AAV5-pCaMKIIα-ChR2 (H134R)-EYFP	UNC Vector Core	N/A
AAV1-EF1a-DIO-hChR2(H134R)-eYFP	UNC Vector Core	N/A
AAV5-pCaMKIIα-GFP	UNC Vector Core	N/A
AAV1-CAG-flex-eGFP-WPRE.bGH	UNC Vector Core	N/A
Chemicals, peptides, and recombinant proteins		
Phosphate buffered saline powder, pH 7.4	Sigma-Aldrich	P38135-10PAK
Paraformaldehyde 4%	Sigma-Aldrich	P6148-1KG
Triton X-100	Sigma-Aldrich	T8787-250ML
Normal Donkey Serum	Merck	S30-100ML
Bovine Serum Albumin	Sigma-Aldrich	A7906-100G
MOWIOL POLYVINYL ALCOHOL	Sigma-Aldrich	81381-250G
SUCROSE $\geq$ 99.5% (GC)	Sigma-Aldrich	S9378-1KG
Potassium Chloride	Sigma-Aldrich	60128-250G-F
Sodium chloride	Chem Supply	SA046-3KG
Calcium Chloride	Sigma-Aldrich	C5080-500G
Sodium phosphate monobasic	Merck	S3139
Sodium Bicarbonate	Sigma-Aldrich	S5761- 1KG
D-(+)-GLUCOSE	Sigma-Aldrich	G7021-1KG
HEPES	Sigma-Aldrich	H3375-250G
Adenosine 5′-triphosphate magnesium salt	Sigma-Aldrich	A9187-500MG
Guanosine 5′-Triphosphate	Sigma-Aldrich	G8877-250MG
Ethanol AR 70%	Sigma-Aldrich	E7023-500ML
Acetic Acid liquid 1%	John Curtin school of Medical Research	N/A
Super-Bond dental cement	Sun Medical, Shiga, Japan	C&B Kit
Experimental Models: Organisms/Strains		
B6.129(Cg)-Cntnap2tm1Pele/J	Jackson	#017482
Shank3tm1.1Pfw/J	Jackson	#018398
B6.129S4-Ptentm1Hwu/J	Jackson	Jax 006440
Emx1-Cre/+ [B6.Cg-Emx1tm1(cre)Krj/J	Jackson	#:005628

Continued

REAGENT or RESOURCE	SOURCE	IDENTIFIER
B6.129P2-Fmr1tm1Cgr/J	Jackson	003025
B6.Cg-Pvalb[tm1(cre)Arbr]	Jackson	#008069
B6.Cg-$Gt(ROSA)26Sor^{tm14(CAG-tdTomato)Hze}$/J	Jackson	#:007914
Software and algorithms		
easyelectrophysiology	easyelectrophysiology	v2.6.4 Pre-release | Easy Electrophys. (easyelectrophysiology.com)
Statview	N/A	N/A
Ethovision	N/A	N/A
Fiji	ImageJ	https://imagej.net/software/fiji/downloads
WinWCP	WinWCP	https://spider.science.strath.ac.uk/sipbs/software_ses.htm
Other		
Fear Conditioning	FEAR-SHUTTLE	Fear-Shuttle - Imetronic
Stereotactic frame	Kopf Instruments	N/A
Optical fiber stubs 2mm	thorlabs	N/A
LED driver system	Thorlabs	LEDD1B T-Cube
Fiber-Coupled LED	Thorlabs	M470F4
Heka LIH-8+8	instruTECH	N/A
Multiclamp 700B	Axon instruments	N/A
vertical P10 puller	Narishige, Japan	N/A
Glass Capillary, Boroscillicate	Clarke Electromedical	GC-150F-15
vibratome VT1200	LEICA	N/A
A1 Confocal	Nikon	N/A

RESOURCE AVAILABILITY

Lead contact

Further information and requests for resources and reagents should be directed to and will be fulfilled by the lead contact, A. Shaam Al Abed (shaam.alabed@anu.edu.au).

Materials availability

This study did not generate new unique reagents.

Data and code availability

- Data reported in this paper will be shared by the lead contact upon request
- This paper does not report original code
- Any additional information required to reanalyze the data reported in this paper is available from the lead contact upon request.

EXPERIMENTAL MODEL AND STUDY PARTICIPANT DETAILS

3 to 5-month-old naive mice were collectively housed in standard Makrolon cages, in a temperature- and humidity-controlled room under a 12 h light/dark cycle (lights on at 07:00), with *ad libitum* access to food and water. We used both males and females to minimize the number of mice produced in this study. WT and *Cntnap2*$^{-/-}$ mice (Jackson ID: #017482[53]) were non-littermates, derived from breeders of the same colony and used for behavior and histological analyses. To mitigate differences between strains that might arise from the rearing environment, we ensured that both strains were housed in the same room, with the same cage content. *Shank 3* KO [Shank3[tm1.1Pfw]/J; Jackson ID: #018398] and littermate controls were kindly provided by Dr Mireille Montcouquiol and Dr Nathalie Sans (Neurocentre Magendie, Bordeaux University, France). *Pten* control (*Pten*$^{F/F}$) and littermate cKO mice (*Pten*$^{F/F}$; *Emx1-Cre/+* [B6.Cg-Emx1tm1(cre)Krj/J]), and *Fmr1* control and KO [B6.129P2-Fmr1tm1Cgr/J; Jackson ID: #003025] mice were male littermates, kindly provided by Dr Andreas Frick (Neurocentre Magendie, Bordeaux University, France). For optogenetics manipulation of PV cells, PV-*Cre* mice (Jackson ID: #008069) were bred with *Cntnap2* $^{-/-}$

mice to obtain *Cntnap2* $^{-/-}$; PV-*Cre*/*Cre* (KO). For electrophysiological recordings, PV-*Cre* (Jackson ID: #008069); *Td-Tomato* mice (control) were bred with *Cntnap2* KO mice to obtain *Cntnap2* $^{-/-}$; PV-Cre/+; Td-Tomato/+ mice (KO).

All experiments took place during the light phase. We replicated the behavioral experiments in two to four different batches. We found no differences in the formation of PTSD-like memory in males and females (Figure S3). Every effort was made to minimize the number of animals used and their suffering. All procedures were conducted in accordance with the European Directive for the care and use of laboratory animals (2010-63-EU) and the animals care guidelines issued by the animal experimental committee of Bordeaux University (CCEA50, agreement number A33-063-099; authorization N°21248), and from the Australian National University Animal Experimentation Ethics Committee (protocol numbers A2018/66, A2020/26, and A2021/43).

METHOD DETAILS

Fear conditioning procedure

PTSD presentation is complex and consists in re-experiencing a threatening event in the form of persistent and intrusive memories, avoidance of reminders of the event, emotional numbing, etc ….[1] However, clinicians consider the unusual nature of the traumatic memory as a cardinal feature of PTSD,[52,54] characterized by both involuntary hypermnesia for some isolated trauma-related stimuli and declarative amnesia for surrounding context.[21] Two methods can be used to attest for PTSD-like memory: (1) **quantitative aspect** of fear memories through the observation of *excessive* responses to stress compared to the behavioral responses of control ("resilient") subjects. (2) the observation of a **qualitative** alteration *specific* to PTSD, i.e.,., hypermnesia and amnesia profile. The present study has selected this option, through this specific feature of PTSD-like memory. In our experiments, this consists of excessive freezing during the tone test (i.e., a salient traumatic cue) and low freezing in the traumatic context.

Habituation (Day 0)

The day before fear conditioning, mice were individually placed for 4 min into a white squared chamber (30 × 15 cm, Imetronic, France) with an opaque PVC floor, in a brightness of 40 lux. The box was cleaned with 1% acetic acid before each trial. This pre-exposure allowed the mice to acclimate and become familiar with the chamber later used for the tone re-exposure test.

Acute Stress

In the "original protocol",[21,22] a 20-min restraint stress was performed immediately after the conditioning. In the modified protocol, we performed a 30-min restraint stress under bright light (100 Lux) 24 h before the conditioning session. Stressed mice were taken to a neutral room and placed into a perforated 50 mL Falcon tube allowing air circulation. Non-stressed control mice were taken to the same room for 20 or 30 min but were kept in their home cage.

Conditioning (Day 1)

Acquisition of fear conditioning was performed in a different context, a transparent squared conditioning chamber (30 × 15 cm) in a brightness of 100 lux, given access to the different visual-spatial cues of the experimental room. The floor of the chamber consisted of 30 stainless-steel rods (5 mm diameter), spaced 5 mm apart and connected to the shock generator. The box was cleaned with 70% ethanol before each trial. All animals were trained with a tone-shock un-pairing procedure, meaning that the tone was non-predictive of the footshock occurrence. This training procedure, fully described in previous studies,[21] promotes the processing of contextual cues in the foreground. Briefly, each animal was placed in the conditioning chamber for 4 min during which it received two tone cues (65 dB, 1 kHz, 15 s) and two foot shocks (squared signal: 0.4 mA, 50 Hz, 1 s), following a pseudo-random distribution. Specifically, animals were placed in the conditioning chamber and receive a shock 100 s later, followed by a tone after a 30s interval. After a 20s delay, the same tone and shock spaced by a 30s interval were presented. Finally, after 20s, mice were returned to their home cage. As the tone was not paired to the footshock, mice selected the conditioning context (i.e., set of static background contextual cues and odor that constitutes the environment in which the conditioning takes place) and not the tone as the correct predictor of the shock (Figure 1A, Day1).

Memory Tests (Day 2)

24 h after conditioning, mice were submitted to two memory retention tests and continuously recorded for offline second-by-second scoring of freezing by an observer blind to experimental groups. Mouse freezing behavior, defined as a lack of movement (except for respiratory-related movements), was used as an index of conditioned fear response.[55] Mice were first submitted to the tone re-exposure test in the safe, familiar chamber during which three successive recording sessions of the behavioral responses were previously performed: one before (first 2 min), one during (next 2 min), and one after (two last minutes) tone presentation (Figure 1A, Day 2). We determined the tone ratio (Insets in the figures) which corresponds to the conditioned response to the tone expressed by the percentage of freezing during tone presentation and compared to the levels of freezing expressed before and after tone presentation (repeated measures on 3 blocks of freezing). This tone ratio was calculated as follows: [% freezing during tone presentation – (% pre-tone period freezing + % post-tone period freezing)/2]/[% freezing during tone presentation + (% pre-tone period freezing + % post-tone period freezing)/2]. 2 h later, mice were submitted to the context re-exposure test. They were placed for 6 min in the conditioning chamber. Freezing to the context was calculated as the percentage

of the total time spent freezing during the successive three blocks of 2 min periods of the test. Optogenetic manipulation of memory formation is detailed below in the optogenetics section of the methods.[22]

Assessment of the persistence of PTSD-like fear memory

To demonstrate that the PTSD-like memory was long-lasting, mice were again submitted to the two memory tests (tone-test and context-test spaced out of 2 h, as in day 2), 20 days after fear conditioning (Figure S1B). To assess generalization of fear, mice were exposed to 2 other tones, i.e., a new tone that is *similar* but not identical to the conditioning tone (3 kHz vs. 1 kHz, respectively), and a white noise (i.e., highly *dissimilar* from the conditioning tone; Figure S1A). We considered fear to be partially generalized when mice were presenting high levels of freezing to the new tone (3 kHz).

Recontextualization was performed as previously described.[22] Briefly, two days after long-term testing (Day 23), mice were re-exposed to the tone cue in the conditioning context, without electric shock (Figures 2A and 2B, **day 23**). This protocol was also performed 3 days after conditioning (Day5), with similar results. The first 2 min of the recontextualization session (pre-tone) allowed us to assess the level of conditioned fear to the conditioning context alone, while the conditioned response to the tone was assessed during the next 2 min, both by the percentage of freezing during the tone presentation and by the tone ratio described above. 24 h later, fear expression was assessed by re-exposing the mice to the regular (i.e., separated from each other) tone and context tests (same tests as in day 2).

Assessment of the core symptoms of ASD

Repetitive behavior

Animals were placed in a cage with clean bedding and recorded for 5 min for offline scoring. The behavior was defined by the percentage of time spent grooming for 2 s minimum, as previously defined[56] and digging.[57]

Social interactions

Following 2 min of habituation in an empty 2-chamber arena, we quantified the time spent close to a novel object or an unfamiliar, sex matched, control mouse for 5 min. The test mouse has access to an unfamiliar object and an unfamiliar mouse contained in a clear plastic box. Preference was quantified when the test mouse was located within a 5 cm-radius around the object/mouse. The results are expressed as the percentage of duration of interactions with the mouse or with the object. Videos were analyzed offline by an experimenter blinded to the experimental conditions. In addition to the main experimental group (stress + fear conditioning (Figures 1H and 1I), we added control groups to ensure the specificity of the effect of traumatic memory on the severity of the core symptoms (i.e., mice were submitted to the stress or the fear conditioning only (Figures S2B–S2G)). Total time spent moving (seconds) was analyzed using Ethovision. Animal path tracking in the social interaction chamber was performed in Ethovision, with separate zones identified for the novel object and novel animal within the arena, and with dynamic threshold detection of the subject animal.[58]

The exacerbation of core symptoms was studied according to the following timeline: Day 1: first assessment of ASD-like behaviors (i.e., social preference and digging/grooming). Day 2–4: fear conditioning. Day 5: second assessment of ASD-like behaviors. Day 6–7: Recontextualization. Day 8: third assessment of ASD-like behavior (Figure 2A).

Long term maintenance of the ASD traits exacerbation was performed 3 weeks after the second assessment; no recontextualization session was performed in this case.

Optogenetic manipulation of the mPFC

Surgery

Mice were injected bilaterally 4 weeks before behavioral experiments with an Adeno-Associated Virus (AAV) to inhibit (*AAV5-pCaMKIIα-ArchT-GFP*, UNC Vector Core) or activate glutamatergic neurons (*AAV5-pCaMKIIα-ChR2 (H134R)-EYFP*, UNC Vector Core) or parvalbumin interneurons (*AAV1-EF1a-DIO-hChR2(H134R)-eYFP*, UNC Vector Core). Control mice were injected with an AAV expressing GFP only (*AAV5-pCaMKIIα-GFP* or *AAV1-CAG-flex-eGFP-WPRE.bGH*, UNC Vector Core). We used glass pipettes (tip diameter 25–35 μm) connected to a picospritzer (Parker Hannifin Corporation) into the mPFC (0.1 μL/site; AP +1.9 mm; L $\pm$ 0.35 mm; DV -1.3 mm). Mice were then implanted with bilateral optic fiber implants, 10 days before behavior (diameter: 200 μm; numerical aperture: 0.39; flat tip; Thorlabs) directed to the mPFC (AP: +1.8 mm, L: $\pm$1.0 mm, DV: -1.3 mm, θ: 10°). Implants were fixed to the skull with Super-Bond dental cement (Sun Medical, Shiga, Japan). Mice were perfused after experiments to confirm correct placements of fibers (Figures S4C, S4D, S4F, and S4G). Viral injections targeted the L2/3 of the mPFC, and virtually all PV-INs in the prelimbic and infralimbic cortices were infected. For optogenetic manipulations, we used an LED (Plexon) at 465 nm with a large spectrum to allow the activation of both ArChT and ChR2. Light was continuously delivered to inactivate the mPFC, and was delivered at 5 Hz (5 ms ON, 195 ms OFF) for mPFC activation of the pyramidal cells (as previously described[22]), and at 10 Hz (10 ms ON, 10 ms OFF) for activation of the parvalbumin interneurons. Mice were submitted to the fear conditioning procedure described above and pyramidal cells of the mPFC were either inhibited or activated during the whole conditioning session. The next day, fear memory was tested as described above. To check the efficiency of the optogenetic activation of the PV-INs in the mPFC, we performed *in vitro* electrophysiological recordings of the pyramidal cells in current-clamp mode at -70 mV (Figures S4H and S4I).

Immunohistochemistry

Animals were perfused transcardially 90 min after the context test on Day 2 for c-Fos analysis, and 60 min after the restraint stress for quantification of Etv1/Er81, and PV, with 0.01M phosphate buffered saline (PBS) to eliminate blood and extraneous material, followed by 4% paraformaldehyde (PFA). Brains were postfixed for 36 h in PFA. Tissues were sectioned at 40 μm using a Leica 1000S vibratome and kept in a cryoprotective ethylene glycol solution at −20°C until processed for immunofluorescence. Sections were first washed and permeabilized in PBS-Triton 0.25%, then non-specific binding sites were blocked by immersing the tissue in 10% normal donkey serum, 2% bovine serum albumin in PBS-Triton 0.25% during 2 h. Tissues were then stained using the primary antibodies overnight: mouse anti-c-Fos (1:1000; Santa Cruz; SC166940), goat anti-PV (1:5000; Swant; PVG-214), rabbit anti-Etv1/Er81 (1:5000; kindly provided by Prof S. Arber, BioZentrum Switzerland), and chicken anti-GFP (1:3000; Aves Labs; GFP-1020). After 3 × 15 min washes, we added anti-rabbit, anti-chicken, anti-mouse, anti-goat Alexa 488 or 555 (1:200; Life Technologies) secondary antibodies for 2 h. After 3 × 15 min washes slices were stain during 10 min with DAPI (5μM; Sigma), mounted on Livingstone slides then covered with Mowiol (Sigma) and coverslip (Thermofisher). c-Fos, PV, and Er81 staining from 2 to 3 slices per animal were imaged using an A1 Nikon confocal fluorescent microscope (20x objective). Stained sections of control and mutant mice were imaged during the same imaging session. Immunofluorescence signals were quantified using the ImageJ (FIJI) software with routine particle analysis procedures (size = 30–500; circularity = 0.30–1.00), to obtain nuclear masks, divided by the area to obtain cell density per mm^2. Er81 and PV expression intensity was quantified in the infralimbic cortex by measuring average fluorescence intensity across each identified cell and normalized to background intensity.

In vitro electrophysiology

Mice were deeply anesthetized with isofluorane 60 min after the restraint stress, or from their homecage, and perfused with ice-cold oxygenated, modified artificial cerebrospinal fluid (ACSF) containing (in mM): 248 sucrose, 3 KCl, 0.5 CaCl2, 4 MgCl2, 1.25 NaH2PO4, 26 NaHCO3, and 1 glucose, saturated with 95% O2 and 5% CO2. The animals were then decapitated, the brain placed in ice-cold oxygenated modified ACSF and 300 μm coronal slices were cut using a Leica 1200S vibratome. Slices were then maintained at room temperature in ACSF containing (in mM): 124 NaCl, 3 KCl, 2 CaCl2, 1 MgCl2, 1.25 NaH2PO4, 26 NaHCO3 and 10 glucose saturated with 95% O2 and 5% CO2. For patch clamp recordings in whole-cell configuration, slices were transferred to a chamber and continuously superfused with ACSF at 32°C. We visualized interneurons located in layer 2–3 of the prefrontal cortex with infrared-differential interference optics through a 40x water-immersion objective. Microelectrodes (6–10 MΩ) were pulled from borosilicate glass (1.5 mm outer diameter x 0.86 inner diameter) using a vertical P10 puller (Narishige, Japan). We used a potassium-gluconate-based intracellular solution containing (in mM): 140 K-gluconate, 10 HEPES, 2 NaCl, 4 KCl, 4 ATP, and 0.4 GTP. Interneurons were kept under current-clamp configuration with an Axoclamp 200A (Axon Instruments) amplifier operating in a fast mode. Data were filtered on-line at 2 kHz, and acquired at a 20 kHz sampling rate of using WinWCP5.5 software (Strathclyde University). Series resistance (Rs) was <25 MΩ upon break-in and Δ Rs < 20% during the course of the experiment. To determine the excitability of the PV + interneurons, we performed 500 ms depolarizing steps of 1 pA and used the first spike evoked by the minimum current needed to elicit an action potential applied from −70 mV. We considered a cell as "delayed" when the first elicited spike at threshold potential occurred more than 24.16 ms (i.e., median in non-stressed controls) after the beginning of the 1 pA depolarizing step.[34] The following parameters were also measured: resting membrane potential (Vrest),membrane resistance, membrane capacitance (Cm), threshold potential for spikes (Vthreshold, defined as dV/dt = 10 mV/ms), rheobase, exponential fit of the slow ramp depolarization that remained just subthreshold during 500 ms current injections, AP amplitude, AP rise and AP duration, after-hyperpolarization (AHP) amplitude and AHP duration. We characterized the changes in membrane potential at near threshold (ΔVm), which corresponds to the activation of the delayed rectifier current (Golomb et al., 2007). We also performed 500 ms depolarizing steps of Δ25pA to determine the maximum firing frequency. Data analysis was performed offline in EasyElectrophysiology (https://www.easyelectrophysiology.com/). Spontaneous excitatory postsynaptic currents (sEPSCs) were recorded in voltage-clamp mode at −70 mV. A stimulating electrode was placed in the cortex to activate cortical fibers and evoke PSCs in layer 2–3 cortical cells. Stimulus delivery was performed by ISO STIM 01D (NPI) and PSCs induced by a train of stimuli (10 Hz, 20 Hz and 40 Hz, 5mA, 30 μs in deep layer V) were recorded in PV + interneurons at −70 mV. For paired-pulse ratio (PPR), EPSC amplitude was measured on 5–10 averaged traces at each inter-pulse interval at the first (EPSC1), second (EPSC2) and fifth event (EPSC5).

QUANTIFICATION AND STATISTICAL ANALYSIS

Data are presented as mean ± SEM. Statistical analyses were performed using the StatView software for 1-way or two-way ANOVA (variable used: genotype; stress groups (fear conditioning (FC) only, FC + stress (PTSD paradigm), or stress only; naive vs. trained for cFos, mouse vs. object exploration), repeated measures were applied where appropriate (within tone or context tests 2 min blocks of freezing (i.e., Pre-Tone, Tone, Post-Tone), test-retests (session 1 vs. session 2 for social/locomotion behaviors). followed by Bonferroni *post-hoc* test or Student's t test, when appropriate. Normality of the data were confirmed using the Kolmogorov-Smirnov test. Statistical significance between cell groups was performed using Chi square test (https://www.socscistatistics.com/). Statistical significance was considered at $p < 0.05$. See Table S1 (Main Figures) and Table S2 (supporting information) for precise *p*-value and tests.